

Internet Electronic Journal of Molecular Design

May 2006, Volume 5, Number 5, Pages 247–259

Editor: Ovidiu Ivanciuc

Special issue dedicated to Professor Lemont B. Kier on the occasion of the 75th birthday

Quantitative *in silico* Analysis of Molecular Recognition and Reactivity of D–Amino Acid Oxidase

Toshihiko Hanai

Health Research Foundation, Institut Pasteur 5F, 103–5 Tanakamonzencho, Sakyo–ku, Kyoto, 606
Japan

Received: March 23, 2006; Accepted: April 20, 2006; Published: May 31, 2006

Citation of the article:

T. Hanai, Quantitative *in silico* Analysis of Molecular Recognition and Reactivity of D–Amino Acid Oxidase, *Internet Electron. J. Mol. Des.* 2006, 5, 247–259, <http://www.biochempress.com>.

Quantitative *in silico* Analysis of Molecular Recognition and Reactivity of D–Amino Acid Oxidase[#]

Toshihiko Hanai *

Health Research Foundation, Institut Pasteur 5F, 103–5 Tanakamonzencho, Sakyo–ku, Kyoto, 606
Japan

Received: March 23, 2006; Accepted: April 20, 2006; Published: May 31, 2006

Internet Electron. J. Mol. Des. 2006, 5 (5), 247–259

Abstract

Computational chemical analysis of enantiomer recognition with chromatography was investigated using molecular mechanics calculations. The method was applied to study enantiomer recognition of the protein D–amino acid oxidase (DAAO). The data for several stereo structures were obtained from databases, and then the substrate was replaced with an amino acid, and the new complexes were optimized using a MM2 calculation to study the conformation of the amino acid complex. Mutant and estimated human DAAO were constructed from the sequence data and the known stereo structure of DAAO. The structures of the new complexes with substituted amino acids were also optimized using MM2 calculations, and used to study selectivity. The reactivity was analyzed based on the atomic distances calculated with MM2, and partial atomic charges calculated with the MOPAC PM5 method. The values of atomic distances and partial atomic charges indicate that the cationic hydrogen of the amino acid could be moved to bind with the anionic nitrogen of flavin. The selectivity of DAAO depends on the initial stereo structure measured by X–ray crystallography and on the amino acid included in the oxidation reaction site. Yeast DAAO has a wider open entrance compared to pig kidney DAAO. The selectivity of the co–enzyme was also analyzed using a computational chemical calculation. The phosphate of flavin mononucleotide (FMN) was caught by a guanidino group of the enzyme, but that of flavin adenine dinucleotide (FAD) was free from ion–ion interaction.

Keywords. D–amino acid; D–amino acid oxidase; FAD; FMN; molecular mechanics; PM5.

Abbreviations and notations

DAAO, D–amino acid oxidase	pac, partial atomic charge
FAD, flavin adenine dinucleotide	FMN, flavin mononucleotide
o–NH ₂ BA, ortho–aminobenzoic acid	LA, lactic acid
TFA, trifluoroacetic acid	

1 INTRODUCTION

Quantitative *in silico* analysis of molecular interactions of fundamental phenomena in nature is very important. It was difficult, however, to use proteins in this type of study. Chromatography is an ideal method to measure the strength of molecular interactions using a variety of standard

[#] Dedicated to Professor Lemont B. Kier on the occasion of the 75th birthday.

* Correspondence author; E–mail: thanai@attglobal.net.

compounds, where molecular size, ionization, and steric hindrance can be determined based on differences in elution time [1]. Except for enantiomer recognition, the computation of molecular docking is, in general, rather simple with chromatography, because a flat model phase can be used. A typical example is the molecular recognition of graphitic carbon [2]. The basic study of molecular docking for quantitative analysis of chromatographic retention using a computational chemical method was applied to the analysis of enantiomer recognition of proteins.

Technically, a variety of enantiomers were separated by chromatography; the major enantiomer recognition phases were Pirkle–type phases, polysaccharide phases, cyclodextrin phases, and protein phases. The mechanism of enantiomer recognition was quantitatively analyzed *in silico*. The technologic advances in computer hardware and software extended the ability to analyze molecular interactions in small to large molecules. Quantitative analysis of enantiomer recognition of Pirkle–type phases was first performed [3,4], and then the enantiomer selective mechanism of alkaloid was analyzed in combination with NMR spectroscopic methods [5].

Proteins naturally recognize enantiomers. The study of protein recognition of enantiomers was applied to analyze the reactivity of D–amino acid oxidase (DAAO), which selectively oxidizes D–amino acids (D–AAs). DAAO was the second flavoenzyme to be discovered. Krebs first detected DAAO activity in tissue specimens in 1935 [6]. This enzyme is present in a variety of organisms, such as bacteria, yeast, fungi, mollusks, insects, fish, amphibians, reptiles, birds, and mammals. Although there is a small difference in the total number of amino acid residues, the amino acid sequences are highly conserved. The physiologic function has been reviewed [7]. The catalytic activity varies for D–AAs. DAAO has broad substrate specificity with a preference for D–AAs bearing hydrophobic side chains of up to four carbon atoms, followed by those carrying polar and aromatic groups [8]. The physiological role, stereo structure, and reaction mechanism of D–amino acid oxidase were reviewed including the mutants [9].

Many crystallographic structures of DAAO are readily available from the Protein Data Bank [10]. The substrates of the DAAO complexes were varied. The substrates were replaced to an amino acid. The conformation of the DAAO–amino acid complex was then optimized using MM2 calculations to analyze which amino acid residue of DAAO was directly involved in the binding, based on various atomic distances and electron transfer which was determined from the partial atomic charge of neighboring atoms. Furthermore, the stereo structure of human DAAO was estimated from the sequence data NP001908 [11] and the stereo structure of pig kidney DAAO 1VE9 [10], because of the similarity of these sequences; and the selectivity of the estimated human DAAO was analyzed. The selectivity of DAAO mutants was also analyzed after docking with various amino acids.

2 EXPERIMENTAL

A Dell Optiplex GX270 computer (Dell, Japan) was used with the CAChe computational program (Fujitsu, Tokyo, Japan). The DAAO data (1COL, 1COK, 1COP, 1AN9, 1VE9, and 1KIF) were downloaded from the RCSB Protein Data Bank [10]. 1COL, 1COK, and 1COP are yeast DAAO with trifluoroacetic acid, lactic acid, and D-alanine (Ala) complexes, respectively. The 1AN9, 1VE9, and 1KIF are pig kidney DAAO with ortho-aminobenzoic acid, benzoic acid, and benzoic acid complexes, respectively. These substrates were replaced with D- or L-Ala to study the conformational change of the initial DAAO. Furthermore, the stereo structure of DAAO mutants was constructed by substituting amino acid residues and optimized using MM2 calculations to study the selectivity of DAAO.

3 RESULTS AND DISCUSSION

The main driving force of protein–drug binding has been studied using a model phase. In the model phase, the ionized drug comes into direct contact with an ion–exchange group located at the bottom of a flowerpot type model phase [12]. Therefore, the main binding force should be an ion–ion interaction between the guanidino group of the protein and the ionized carboxyl group of the alanine. The original molecule included in the stereo structure of DAAO was replaced with an amino acid by superimposing of these carboxyl groups. Ionization is also necessary for the binding mechanism [13]. The molecular form of alanine was also used for the calculation to study the effect of ionization. The stereo structure of these DAAO and alanine complexes was optimized using the MM2 molecular mechanics calculation of the CAChe program.

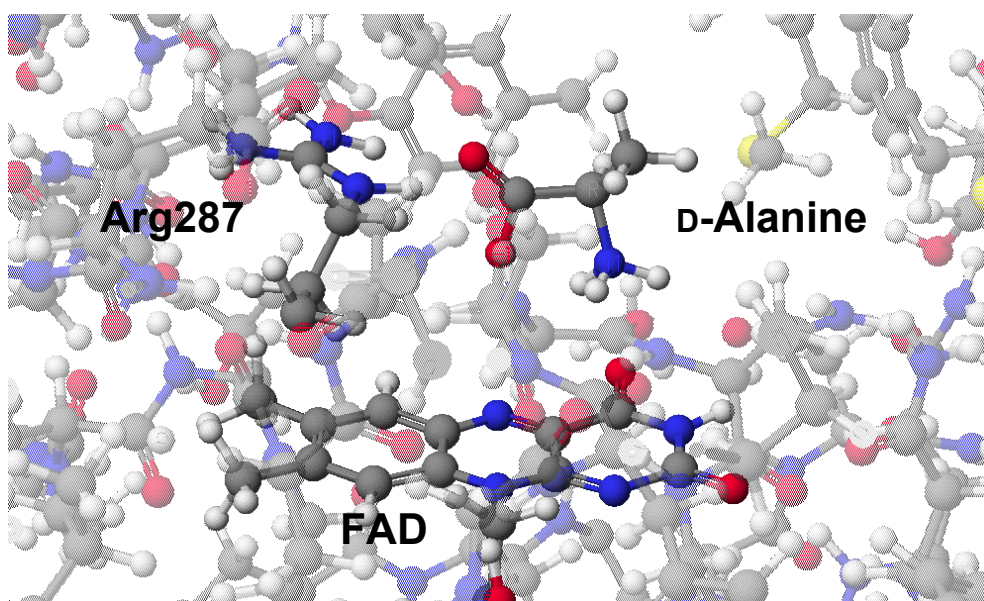


Figure 1. Conformation of D-Alanine with Arg287 of 1COL (DAAO).

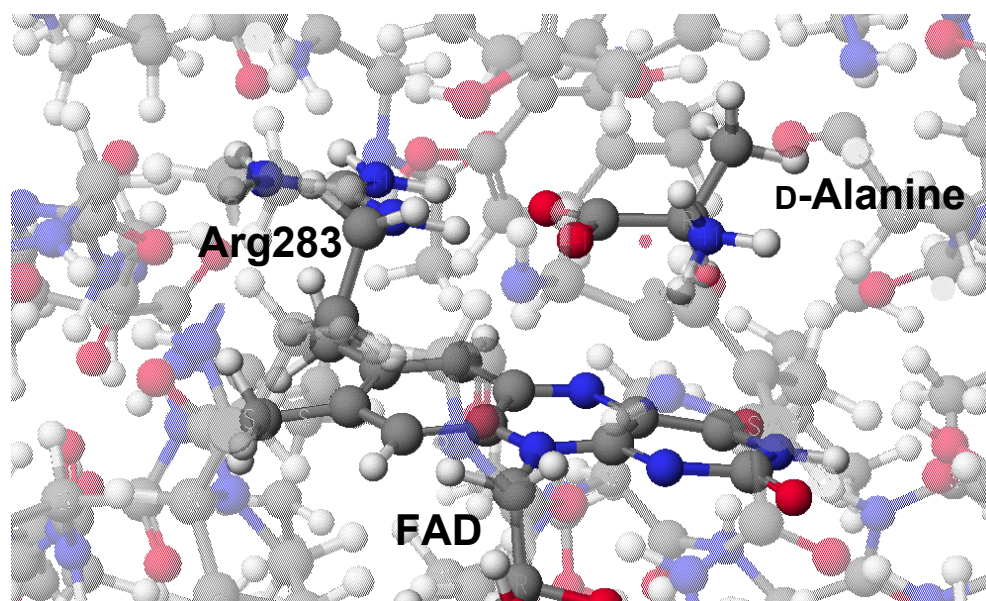


Figure 2. Conformation of D-Alanine with Arg283 of Human DAAO.

The conformation depended on downloaded DAAO structures (see in Figures 1 and 2), in which D-Ala and surrounding amino acid residues were selected and locked for the PM5 calculation of the CAChe program. The details of the difference can be understood from their atomic distances and partial atomic charges (summarized in Tables 1 and 2). 1COL and the ionized D-Ala complex is shown in Figure 1 and an estimated human DAAO and D-Ala complex is shown in Figure 2.

Table 1. Atomic Distance (Å) of the Complex for Several DAAO Data

Complex	C1–C2	C2–N1	O1–N3	O1–N4	O2–N2	O2–N3	O2–N4	N1–O3	N1–O4
1COL TFA(S) ion	1.628	1.488	4.902	5.232	3.955	3.281	3.327	3.740	3.166
1COL D-Ala ion	1.486	1.494	2.946	3.263	3.201	4.181	4.016	3.037	3.016
1COL L-Ala ion	1.481	1.488	2.944	3.067	2.780	4.568	4.601	4.906	6.675
1COP D-Ala ion	1.561	1.511	3.078	3.492	3.796	3.217	3.424	2.795	5.979
1COK LA ion	1.561	–	3.073	2.493	4.089	4.956	3.474	–	–
1COK D-Ala ion	1.478	1.487	2.937	2.947	4.328	4.229	3.017	2.230	4.972
1COK L-Ala ion	1.484	1.477	2.991	2.917	4.095	4.232	2.914	5.497	5.637
1AN9 o-NH2BA ion	1.517	1.465	2.868	3.408	3.063	3.957	3.775	2.775	3.351
1AN9 D-Ala ion	1.493	1.495	2.979	3.044	3.755	4.266	3.101	2.276	3.012
1AN9 L-Ala ion	1.482	1.485	2.884	2.968	3.303	4.207	3.046	5.210	6.364
1K1F D-Ala ion	1.475	1.487	2.686	2.883	3.499	4.596	4.528	2.454	2.440
1VE9 BA ion	1.498	–	2.801	2.401	2.852	4.751	3.613	–	–
1VE9 D-Ala ion	1.492	1.494	2.969	3.048	3.715	4.283	3.140	2.257	3.020
1VE9 L-Ala ion	1.478	1.489	2.894	2.992	3.351	4.115	3.041	5.496	6.597
Human D-Ala ion	1.488	1.492	2.932	3.075	3.826	3.626	3.027	2.264	2.911
D-Ala mol	1.563	1.456							
D-Ala ion	1.418	1.470							

TFA: trifluoroacetic acid

LA: lactic acid

o-NH2BA: ortho-aminobenzoic acid

BA: benzoic acid

mol: molecular form, ion: ionic form

For the location of atoms N, O, H: see Figure 3

Table 1. (Continued)

Complex	N1–O5	N1–O6	N1–O8	N3–O6	N3–O7	N4–O6	N4–O7	O6–O7	H1–N2	N1–O3a
1COL TFA(S) ion	2.998	5.316	–	2.667	2.298	2.613	4.367	3.908	5.329	4.687
1COL D–Ala ion	2.273	5.206	–	3.502	2.294	2.704	4.343	5.016	5.575	3.793
1COL L–Ala ion	6.286	2.471	–	2.625	2.296	2.662	4.280	3.475	5.346	2.990
1COP D–Ala ion	4.251	4.765	–	4.325	2.305	3.676	4.205	4.697	3.373	3.114
1COK LA ion	–	–	–	2.638	2.838	2.640	4.271	3.137	4.677	–
1COK D–Ala ion	4.707	4.570	–	2.655	2.823	2.632	4.252	3.161	2.557	4.470
1COK L–Ala ion	5.452	3.035	–	2.710	2.962	2.734	4.370	3.107	2.368	6.309
1AN9 o–NH2BA ion	4.252	2.954	3.269	6.200	2.368	5.146	4.889	7.681	–	–
1AN9 D–Ala ion	4.843	2.888	2.460	5.956	2.468	5.053	4.585	7.799	2.793	–
1AN9 L–Ala ion	5.210	4.440	5.983	6.583	2.348	5.673	4.443	7.799	2.404	–
1K1F D–Ala ion	5.036	2.871	2.430	5.104	3.254	4.860	4.668	8.041	5.229	–
1VE9 BA ion	–	–	–	6.490	2.265	5.561	3.933	7.415	–	–
1VE9 D–Ala ion	5.006	2.910	2.477	5.601	2.559	4.657	4.657	7.546	3.100	–
1VE9 L–Ala ion	5.835	4.211	5.940	6.774	2.313	5.694	4.335	7.917	2.922	–
Human D–Ala ion	4.825	2.903	2.441	5.622	2.308	4.685	4.364	6.588	2.988	–

Table 2. Partial Atomic Charge of Targeted Atoms

Complex	C1	C2	O1	O2	O3	O4	O5	O6
1COL TFA(S) ion	0.494	–0.421	–0.450	–0.658	–0.424	–0.526	–0.415	–0.456
1COL D–Ala ion	0.432	–0.221	–0.638	–0.644	–0.492	–0.523	–0.449	–0.421
1COL L–Ala ion	0.450	–0.255	–0.666	–0.606	–0.573	–0.560	–0.443	–0.398
1COP D–Ala ion	0.431	–0.200	–0.659	–0.602	–0.574	–0.497	–0.388	–0.440
1COK LA ion	0.401	0.033	–0.690	–0.614	–0.470	–	–0.419	–0.400
1COK D–Ala ion	0.437	–0.200	–0.606	–0.677	–0.555	–0.471	–0.371	–0.428
1COK L–Ala ion	0.443	–0.220	–0.733	–0.533	–0.480	–0.473	–0.389	–0.419
1AN9 o–NH2BA ion	0.475	–0.105	–0.608	–0.698	–0.461	–0.489	–0.406	–0.417
1AN9 D–Ala ion	0.448	–0.203	–0.601	–0.709	–0.477	–0.501	–0.391	–0.416
1AN9 L–Ala ion	0.448	–0.287	–0.723	–0.556	–0.416	–0.458	–0.439	–0.390
1K1F D–Ala ion	0.460	–0.218	–0.647	–0.664	–0.528	–0.497	–0.447	–0.408
1VE9 BA ion	0.502	–0.155	–0.695	–0.631	–0.420	–0.442	–0.423	–0.413
1VE9 D–Ala ion	0.452	–0.208	–0.594	–0.710	–0.464	–0.497	–0.389	–0.430
1VE9 L–Ala ion	0.436	–0.222	–0.717	–0.556	–0.406	–0.440	–0.418	–0.393
Human D–Ala ion	0.447	–0.200	–0.601	–0.706	–0.459	–0.405	–0.389	–0.441
D–Ala ion or FAD	0.468	–0.318	–0.504	–0.601	–0.500	–0.454	–0.364	–0.364

	O7	O8	N1	N2	N3	N4	H1	O3a
1COL TFA(S) ion	–0.417	–	0.048	0.019	–0.436	–0.285	0.264	–0.461
1COL D–Ala ion	–0.405	–	0.021	0.013	–0.444	–0.266	0.191	–0.456
1COL L–Ala ion	–0.396	–	0.053	–0.046	–0.467	–0.296	0.189	–0.422
1COP D–Ala ion	–0.441	–	0.025	–0.014	–0.457	–0.279	0.204	–0.453
1COK LA ion	–0.398	–	–	–0.018	–0.478	–0.282	0.091	–0.445
1COK D–Ala ion	–0.400	–	0.035	–0.014	–0.471	–0.263	0.225	–0.428
1COK L–Ala ion	–0.404	–	0.010	–0.033	–0.472	–0.253	0.231	–0.432
1AN9 o–NH2BA ion	–0.420	–0.512	0.064	–0.010	–0.441	–0.278	–	–
1AN9 D–Ala ion	–0.421	–0.419	0.010	–0.031	–0.430	–0.274	0.179	–
1AN9 L–Ala ion	–0.407	–0.414	0.028	–0.064	–0.457	–0.265	0.183	–
1K1F D–Ala ion	–0.413	–0.427	0.009	–0.042	–0.448	–0.263	0.172	–
1VE9 BA ion	–0.423	–0.437	–	–0.022	–0.446	–0.316	–	–
1VE9 D–Ala ion	–0.419	–0.414	0.014	0.000	–0.439	–0.276	0.183	–
1VE9 L–Ala ion	–0.407	–0.471	0.024	–0.043	–0.456	–0.275	0.209	–
Human D–Ala ion	–0.415	–0.510	0.043	0.007	–0.447	–0.267	0.178	–
D–Ala or FAD	–0.422	0.054	0.054	0.016	–0.499	–0.273	0.178	–

See Table 1 for symbols.

Ionization of the carboxyl group shortens the atomic distance and changes the atom partial charge value to favor the connection. The atomic distance of the ionized form of alanine between C(1) and C(2) was less than that of the molecular form, but the distance increased slightly by forming a complex with DAAO. The atomic distance between the carboxyl group of the alanine and the guanidino group of the arginine (Arg)283 or 287 indicated that the ion–ion interaction had a different configuration. The ion–ion interaction form was parallel in 1COK, 1AN9, and 1VE9, but perpendicular in 1COL, 1COP, and 1KIF. This finding indicated that selection of an original stereo structure is very important for further docking studies. The initial structure of the DAAO did not have the same conformation when replaced with D–Ala, which might be due to elimination of water molecules prior to this calculation. This is a potential limitation of the present calculation method. The conformation difference was further analyzed based on the atomic distance and partial atomic charge of the target amino acid residue and substrate. The target atoms are shown in Figure 3. The amino acid residues of yeast DAAO are asparagine (Asn)56, tyrosine (Tyr)225, Tyr240, Arg287, and serine (Ser)337; and those of pig kidney DAAO are glutamine (Glu)53, proline (Pro)54, Tyr224, Tyr 228, Arg283, and glycine (Gly)313.

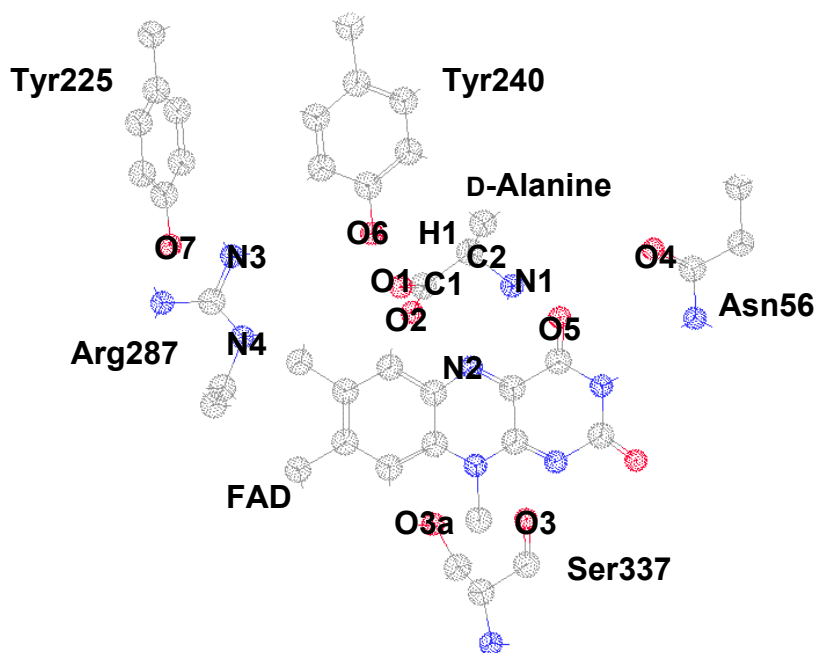


Figure 3. Selected atoms of D–Alanine and 1COP (DAAO) complex.

The target atoms are indicated in Figure 3 as O(3) of Asn56 and O(4) of Ser337, and O(5) of FAD for yeast DAAO (1COP, 1COL, 1COK) and O(3) of Gly313, O(4) of Glu53, O(5) of FAD, and O(8) of Pro54 for pig kidney DAAO (1AN9, 1VE9, 1KIF) and human DAAO.

After docking of D– or L–Ala with the 1COL protein, the atomic distance between the C(2) carbon and N(1) nitrogen increased slightly. The ionized O(2) oxygen of the carboxyl group shifted

toward the N(2) nitrogen of the flavin adenine dinucleotide (FAD). The O(1) oxygen moved toward the guanidino group of Arg287, but the O(2) oxygen moved away from the guanidino group. These phenomena indicate that the ion–ion interactions were perpendicular, and not parallel. When an amino acid was unlocked, the amino acid shifted toward the guanidino group. This shift affected the atomic distance between the ionized amino group and the counter O(3) carbonyl group of Ser337, O(4) of Asn56, and O(5) of FAD. The hydroxy group of Tyr225 and 240 formed a hydrogen bond with the guanidino group of Arg287. Tyr240 acts as a lid, which swings between the open and closed conformations to allow access to amino acids [14]. The amino group of the molecular form of L-Ala formed a hydrogen bond with the hydroxy group of Tyr240. This shift occurred inside a small cage constructed by neighboring locked amino acid residues whose initial conformation was optimized as whole DAAO using MM2. It is not clear whether a further shift occurred *in vivo*. Therefore, the above discussion is based on their initially optimized structure.

The high-resolution structures of yeast DAAO complexes with D-Ala (1COP), D-trifluoroacetic acid (1COL), and lactic acid (1COK) provided strong evidence for hydride transfer as the mechanism of dehydrogenation [15]. Their conformation with D-Ala, however, was different in this experiment and it did not support the proposed mechanism.

The conformation of pig kidney DAAO is similar, even if the original structure holds a molecule other than 1KIF. The guanidino group of Arg287 and the carboxyl group of D-Ala form a parallel interaction. The ionized amino group of D-Ala contacts the O(3) of Gly313 and the O(4) of Glu53, and then the O(8) of Pro54. H(1) contacts N(2) directly. The H(1)–N(2) distance is less than 3 Å and N(1)–O(5) was approximately 5 Å. 1COP and 1COL demonstrated different conformations in which the N(1)–O(5) distance was shorter and H(1)–N(2) distance was longer. There is a significant difference in the location of Tyr224 and Tyr240. The Tyr240 of yeast DAAO shifts toward the guanidino group of Arg287 and opens the reaction chamber. Tyr224 is located at a similar position. This result can be understood from the O(6)–O(7) distance. The partial atomic charge of N(1) and H(1) of pig kidney DAAO is less than that of yeast DAAO. The strong partial atomic charge N(3) of yeast DAAO supports the shift. The carboxyl group of L-Ala binds strongly with the counter guanidino group of arginine, and should prevent the binding of D-Ala. The L-Ala amino group, however, is far from the O(5) of flavin and the O(3) of Ser337 or Gly313, and closer to O(6) of Tyr240. The conformation of the hydrogen bonding type interaction of the alanine amino group and carbonyl groups varies with the type of DAAO.

The partial atomic charge of C(2) and H(1) was cationic, and that of the counter atom N(2) of flavin was anionic compared to their original values. The partial atomic charge of N(1) and O(5) was anionic. These results were not related to their atomic distance. The atomic distance and partial atomic charge indicated that H(1) was transferred to the N(2) of flavin. C(1) was cationic. These results did not support the common reaction mechanisms. Therefore, further study was performed

mainly using 1COP. The important indicators of their oxidation process are the atomic distance between the N(1) of alanine and the counter oxygens, and the change in their partial atomic charge.

The hydroxy group of tyrosine affected the docking substrate to form an ion–ion interaction. The effect of the amino acid was further analyzed to evaluate the ability of the surrounding amino acid residues to trap the alanine. The extracted residues formed a cage to trap an ionized D-Ala as shown in Figure 4. The key atomic distance and the related partial atomic charge were obtained after step-by-step amino acid residue removal and optimized using a PM5 calculation. The results are summarized in Table 3.

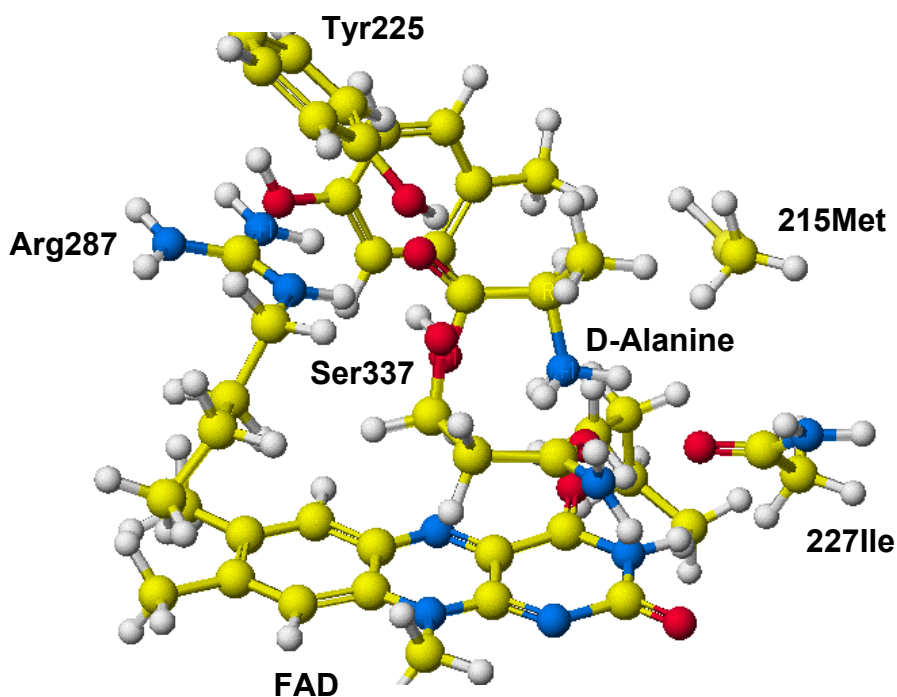


Figure 4. Surrounding amino acid residues and FAD of 1COP DAAO.

Table 3. Atomic Distance (AD) and Partial Atomic Charge (PAC) of Extracted 1COP

Sample / AD	C(1)–C(2)	C(2)–N(1)	H(1)–N(2)	N(1)–O(5)	O(2)–N(2)
1COP-7 ^a	1.619	1.510	4.155	2.953	3.079
1COP-6 ^b	1.587	1.516	4.324	4.070	3.511
1COP-5 ^c	1.576	1.516	3.528	4.397	3.708
1COP-3 ^d	1.578	1.513	3.486	4.185	3.498
1COP ^e	1.561	1.511	3.373	4.251	3.796

Sample / PAC	C(1)	C(2)	N(1)	H(1)	N(2)	O(5)	O(2)
1COP-7 ^a	0.472	-0.291	0.047	0.175	-0.065	-0.488	-0.636
1COP-6 ^b	0.440	-0.241	0.042	0.192	-0.026	-0.410	-0.591
1COP-5 ^c	0.414	-0.214	0.046	0.195	-0.013	-0.397	-0.633
1COP-3 ^d	0.450	-0.217	0.044	0.206	-0.008	-0.400	-0.594
1COP ^e	0.431	-0.200	0.025	0.204	-0.014	-0.388	-0.602

^a: original – Asn56, Phe60, Met215, Tyr225, Tyr240, Arg287, and Ser337; ^b: original – Asn56, Phe60, Met215, Tyr225, Tyr240, Ser337; ^c: original – Asn56, Phe60, Met215, Tyr225, Tyr240; ^d: Asn56, Phe60, Met215; ^e: original extracted conformation of 1COP

Removing the amino acid residues resulted in an increase in the atomic distance of C(1)–C(2), H(1)–N(2), but a decrease in the atomic distance of N(1)–O(5) and O(2)–N(2). The absolute value of the partial atomic charge of C(2), N(1), N(2), O(5) increased and that of H(1) decreased. The change in these values indicates a complex conformation between flavin and ionized D–Ala. Arg287 and Ser337 are key residues for maintaining ionized D–Ala at the reaction site. The cavity size was affected by the surrounding amino acid residues, and should affect the complex conformation. This effect also depends on the size of the amino acid being oxidized. The free movement of the substrate (D–AA) favors the carbanion mechanism based on the partial atomic charge of C(2). N(2) was anionic, however, and the H(1)–N(2) distance increased. This model experiment did not provide a clear answer for the reaction mechanism. That is, the determination of the reaction mechanism depends upon the flexibility of the DAAO protein optimized by the computational chemical calculation. This conclusion is also supported by the different conformations of the arginine guanidino group and amino–acid carboxyl group complex constructed from different crystallographic structures.

Table 4. Atomic Distance (Å) of Complex With Mutants. See Figure 3 for Atom Identification.

Complex	C1–C2	C2–N1	O1–N3	O1–N4	O2–N2	O2–N3	O2–N4	N1–O3	N1–O4
1COP D–Ala mol	1.513	1.448	3.058	2.748	4.503	3.080	4.211	2.943	5.104
1COP D–Ala ion	1.561	1.511	3.078	3.492	3.796	3.217	3.424	2.795	5.979
1COP L–Ala mol	1.519	1.445	2.654	2.623	5.508	3.046	3.176	5.800	5.801
1COP L–Ala ion	1.482	1.498	2.813	4.151	6.267	2.938	2.999	8.293	10.398
1COPM215R D–Ala mol	1.520	1.445	2.940	2.986	3.804	4.326	3.042	3.297	6.125
1COPM215R D–Ala ion	1.464	1.487	3.000	3.677	4.774	2.812	2.787	2.243	6.556
1COPM215R D–Pro ion	1.458	1.490	5.007	4.756	4.484	2.992	3.011	3.797	4.716
1COPM215R D–Asp ion	1.475	1.497	2.896	3.010	2.864	4.615	3.754	4.975	6.820
1COPL120H D–Ala mol	1.522	1.447	2.973	2.972	3.800	4.364	3.056	3.365	6.008
1COPL120H D–Ala ion	1.484	1.493	2.892	3.964	3.863	3.047	3.021	2.257	6.270
1COPL120R D–Pro ion	1.467	1.488	4.506	3.378	4.694	2.944	2.925	2.418	6.042
1COPL120H D–Asp ion	1.473	1.505	2.955	3.983	3.969	3.057	2.730	2.339	5.298

Complex	N1–O5	N1–O6	N3–O6	N3–O7	N4–O6	N4–O7	O6–O7	H1–N2	N1–O3a
1COP D–Ala mol	3.285	4.417	4.328	3.661	5.139	5.431	4.983	2.442	5.088
1COP D–Ala ion	4.251	4.765	4.325	2.305	3.676	4.205	4.697	2.373	3.114
1COP L–Ala mol	3.966	6.215	3.475	2.310	2.751	4.340	4.704	2.502	5.390
1COP L–Ala ion	8.484	2.453	5.215	2.458	6.951	3.616	6.442	6.090	6.314
1COPM215R D–Ala mol	3.388	4.856	2.613	2.633	2.614	4.288	3.158	3.571	4.906
1COPM215R D–Ala ion	4.905	4.835	2.569	2.312	2.685	4.216	3.233	2.704	2.403
1COPM215R D–Pro ion	2.404	4.963	2.609	2.783	2.643	4.260	3.192	4.917	4.305
1COPM215R D–Asp ion	2.268	4.907	3.712	2.993	2.589	4.443	4.886	4.379	6.304
1COPL120H D–Ala mol	3.307	4.861	2.576	2.770	2.617	4.276	3.113	3.520	4.979
1COPL120H D–Ala ion	4.724	4.135	2.662	2.378	2.507	4.430	4.078	2.821	2.372
1COPL120R D–Pro ion	4.592	4.662	2.661	2.796	2.678	4.230	3.165	2.996	4.268
1COPL120H D–Asp ion	3.958	4.329	4.328	3.661	5.139	5.431	4.983	2.183	4.321

A molecular mechanics simulation for the DAAO–D–leucine complex was performed to obtain a model for the enzyme–substrate complex. According to the enzyme–amino acid complex model, H(1) points toward the flavin N(2) while the amino group can approach the O(3) of Gly313 and the O(5) of flavin. This model enables the evaluation of the amino acid–flavin interaction prior to

electron transfer from the amino acid to flavin and suggests two possible mechanisms for the reductive–half reaction of DAAO, the electron–proton–electron transfer mechanism and the ionic mechanism [16]. This approach might work for 1COK, 1AN9, and human DAAO due to the less than 3 Å distance between H(1)–N(1), but not for the 1VE9 complex. These four complexes form a parallel ion–ion interaction between the carboxyl group of D-Ala and the guanidino group of Arg283 or 287.

Table 5. Partial Atomic Charge of Targeted Atoms. See Table 1 for Atom Identification.

Complex	C1	C2	O1	O2	O3	O4	O5	O6
1COP D-Ala mol	0.345	-0.036	-0.517	-0.408	-0.492	-0.508	-0.444	-0.415
1COP D-Ala ion	0.431	-0.200	-0.659	-0.602	-0.574	-0.497	-0.388	-0.440
1COP L-Ala mol	0.358	-0.005	-0.437	-0.403	-0.429	-0.510	-0.394	-0.395
1COP L-Ala ion	0.440	-0.226	-0.622	-0.607	-0.426	-0.490	-0.392	-0.430
1COPM215R D-Ala mol	0.405	-0.028	-0.467	-0.383	-0.489	-0.490	-0.476	-0.447
1COPM215R D-Ala ion	0.452	-0.203	-0.641	-0.661	-0.539	-0.518	-0.417	-0.458
1COPM215R D-Pro ion	0.467	-0.206	-0.597	-0.648	-0.483	-0.504	-0.526	-0.440
1COPM215R D-Asp ion	0.435	-0.190	-0.650	-0.639	-0.491	-0.453	-0.474	-0.432
1COPL120H D-Ala mol	0.407	-0.020	-0.477	-0.387	-0.471	-0.472	-0.430	-0.442
1COPL120H D-Ala ion	0.450	-0.208	-0.591	-0.706	-0.526	-0.499	-0.377	-0.466
1COPL120H D-Pro ion	0.463	-0.229	-0.660	-0.625	-0.502	-0.490	-0.432	-0.433
1COPL120H D-Asp ion	0.462	-0.184	-0.605	-0.738	-0.503	-0.450	-0.378	-0.395
FAD	–	–	–	–	-0.500	-0.454	-0.364	-0.364
D-Ala mol	0.285	0.002	-0.433	-0.383	–	–	–	–
D-Ala ion	0.468	-0.318	-0.504	-0.601	–	–	–	–
D-Pro ion	0.467	-0.299	-0.601	-0.514	–	–	–	–
D-Asp ion	0.480	-0.347	-0.507	-0.579	–	–	–	–

	O7	N1	N2	N3	N4	H1	O3a
1COP D-Ala mol	-0.410	-0.363	-0.019	-0.429	-0.325	0.202	-0.438
1COP D-Ala ion	-0.441	0.025	-0.014	-0.457	-0.279	0.204	-0.453
1COP L-Ala mol	-0.416	-0.428	-0.044	-0.455	-0.270	0.116	-0.426
1COP L-Ala ion	-0.413	0.000	-0.023	-0.434	-0.261	0.192	-0.464
1COPM215R D-Ala mol	-0.403	-0.421	-0.011	-0.470	-0.292	0.169	-0.432
1COPM215R D-Ala ion	-0.425	0.030	-0.021	-0.475	-0.281	0.202	-0.464
1COPM215R D-Pro ion	-0.398	0.089	0.014	-0.474	-0.274	0.208	-0.464
1COPM215R D-Asp ion	-0.399	-0.004	-0.039	-0.471	-0.249	0.198	-0.451
1COPL120H D-Ala mol	-0.403	-0.426	-0.008	-0.470	-0.288	0.183	-0.433
1COPL120H D-Ala ion	-0.436	0.022	-0.008	-0.465	-0.287	0.209	-0.451
1COPL120H D-Pro ion	-0.408	0.217	-0.026	-0.467	-0.264	0.217	-0.429
1COPL120H D-Asp ion	-0.434	0.005	0.002	-0.394	-0.341	0.199	-0.444
FAD	-0.422	–	0.016	-0.499	-0.273	–	–
D-Ala mol	–	-0.389	–	–	–	0.163	–
D-Ala ion	–	0.054	–	–	–	0.178	–
D-Pro ion	–	0.065	–	–	–	0.173	–
D-Asp ion	–	0.070	–	–	–	0.208	–

The selectivity of DAAO was further studied using the mutants M213R [17] and L118H [18] with selected D-amino acids such as D-Ala, D-Pro, and D-Asp, which are yeast DAAO mutants in which the amino acid access is wider than that of pig kidney DAAO. These mutants were prepared to develop a selective D-amino acid analyzer, especially D-Ala, D-Asp, and D-Glu, which are formed during food processing and also originate from microbial sources, including water, soil, and

other environments, and might be ingested by humans. Their content is proposed to be a reliable molecular marker of ripening and an index of food product quality [18]. The M215R mutant oxidized both the neutral and acidic D-AAAs [17]. The L120H DAAO mutant response had a limited dependence on the mixture composition [18]. Their stereo structure was constructed based on the stereo structure of 1COP. D-Pro was selected as the most reactive amino acid [8], and D-Asp was selected as an acidic amino acid [17, 18]. Atomic distance and partial atomic charge of selected atoms are given in Tables 4 and 5.

The significant difference in the adsorption of D-Ala was the location of Tyr240 that moved toward Arg287 and increased the size of the entrance in both M215R and L120H mutants. The difference in selectivity between M215R and L120H mutants was due to the atomic distance N(1)–O(5) and H(1)–N(2) of their D-Pro and D-Asp complexes. N(1)–O(5) was short in M215R and H(1)–N(2) was short in L120H. The ion–ion interaction conformation between the guanidino group of arginine and the carboxyl group of the amino acid varied depending on the complex. The parallel interaction form was observed for the M215R–D-Ala, L120H–D-Ala, and L120H–D-Asp complexes, and the perpendicular form was observed for M215R–D-Pro, M215–D-Asp, and L120H–D-Pro complexes. The partial atomic charge of C(2) and H(1) was cationic, but that of O(5) and N(2) was anionic; that of H(1) was cationic except D-Asp, and that of N(2), which is an acceptor of H(1) was anionic. These results did not provide a clear answer to the reaction mechanism. In particular, the N(1)–O(5) distance of M215R was very short, and this result supports the sensitive oxidation of D-Asp [16]. Asn56 O(4) and Ser337 O(3a) did not contribute to holding D-Asp and D-Pro. The partial atomic charge indicated that D-Pro is more easily oxidized than D-Ala, as previously reported [8]. H120 of L120H pushed Arg97 closed to D-Ala or D-Asp, but Phe60 exists between the amino acid and the guanidino group of Arg97. It is not clear whether the conformation changed to favor an ion–ion interaction between a carboxyl group of D-amino acid and the guanidino group of Arg97 *in vivo* or not.

Studies of DAAO indicated that the few conserved residues of the active site do not have a role in acid–base catalytic activity, but rather are involved in substrate interactions. The striking absence of essential residues acting in acid–base catalysis and the mode of substrate orientation in the active site, taken together with the results of free energy correlation studies, support a hydride transfer type of mechanism [20]; however, the above computational chemical analysis did not support this conclusion due to the cationic carbon C(2) and hydrogen H(1).

Further studies were performed to examine the lack of catalytic activity of the flavin mononucleotide (FMN) using 1COP. The FMN-bound 1COP was constructed from the original 1COP after removing the extra adenosine monophosphate from FAD, then the structure was optimized using MM2, and the partial atomic charge was calculated using PM5. The calculated atomic distance and partial atomic charge are summarized in Table 6.

Table 6. Selectivity of FAD and FMN

Atomic Distance (Å)							
Complex	N2–O3	N2–O6	N2–O7	N2–O4	N3–O6	N3–O7	
FMN	4.260	5.263	7.000	6.148	2.735	2.286	
FAD	4.862	6.595	4.919	7.091	4.328	3.662	

Partial Atomic Charge							
Complex	N2	N3	O3	O4	O5	O6	O7
FMN	–0.017	–0.452	–0.463	–0.511	–0.427	–0.427	–0.414
FAD	0.016	–0.499	–0.500	–0.454	–0.364	–0.364	–0.422

There was a significant difference in the cavity size. The adenine moiety interacted with the backbone of the amino acid residues and to bind with FAD [20], leading to a tight interaction. The flavin of FMN, however, was directed into the reaction chamber. In addition, the partial atomic charge of N(2) and O(5) of FMN are very anionic compared to those of FAD. Another possibility is FMN is not buried in DAAO. Enzymes such as pentaerythritol tetranitrate reductase (1GVO), pentaerythritol tetranitrate reductase W102Y mutant (1VYS), and reduced pentaerythritol tetranitrate reductase (1H63) depending on FMN locate a guanidino group near by the phosphate [10], and FMN is held at the location by an ion–ion interaction.

4 CONCLUSIONS

Computational chemical analysis of enantiomer recognition with chromatography was investigated using molecular mechanics calculations. The method was applied to study enantiomer recognition of the protein D-amino acid oxidase (DAAO). The data for several stereo structures were obtained from databases, and then the substrate was replaced with an amino acid, and the new complexes were optimized using a MM2 calculation to study the conformation of the amino acid complex. Mutant and estimated human DAAO were constructed from the sequence data and the known stereo structure of DAAO. The structures of the new complexes with substituted amino acids were also optimized using MM2 calculations, and used to study selectivity.

Tyrosine acts as a lid located above a trapped amino acid in pig kidney DAAO, but the tyrosine shifts toward arginine and opens the cavity entrance in yeast DAAO. This means that catalytic activity and selectivity in pig kidney DAAO are limited. The computational chemical analysis indicated a different stereo selectivity and complex formation. The reaction mechanism, however, was not clearly defined from these results. Yeast origin DAAOs did not have the same conformation, and suggested the possibility of different reaction mechanisms. Further study is necessary to model the flexibility of protein structures *in vivo* for enzyme activity.

Acknowledgment

The authors thanks Dr. M. Maeda, School of Pharmaceutical Sciences, Kitasato University for helpful discussions.

5 REFERENCES

- [1] T. Hanai, (Ed) *HPLC, A Practical Guide*, RSC Press, Cambridge, 1999.
- [2] T. Hanai, Analysis of the mechanism of retention on graphitic carbon by a computational chemical method, *J. Chromatogr. A*, **2004**, 1030, 13–16.
- [3] K. B. Lipkowitz, Atomistic modeling of enantioselection: Applications in chiral chromatography, *Theoret. Comput. Chem.* **1998**, 5, 329–379.
- [4] T. Hanai, H. Hatano, N. Nimura, and T. Kinoshita, Computational chemical analysis of chiral recognition in liquid chromatography, selectivity of *N*-(*R*)-1-(α -naphthyl)ethylaminocarbonyl-(*R* or *S*)-valine and *N*-(*S*)-1-(α -naphthyl)ethylaminocarbonyl-(*R* or *S*)-valine bonded aminopropyl silica gel, *Anal. Chim. Acta*, **1996**, 332, 213–224.
- [5] C. Czerwenka, M. M. Zhang, H. Kahlig, N. M. Maier, K. B. Lipkowitz, and W. Lindner, Chiral recognition of peptide enantiomers by cinchona alkaloid derived chiral selectors: mechanistic investigations by liquid chromatography, NMR spectroscopy, and molecular modeling, *J. Org. Chem.* **2003**, 68, 8315–27.
- [6] H. A. Krebs, (1935) Metabolism of amino acids III. Determination of amino acids, *Biochem. J.* **1935**, 29, 1620–1644.
- [7] R. Konno and Y. Yasumura, D-Amino-acid oxidase and its physiological function, *Int. J. Biochem.* **1992**, 24, 519–524.
- [8] D. Malcolm and K. Kjell, D-Amino acid oxidase II, Specificity, competitive inhibition and reaction sequence, *Biochem. Biophys. Acta*, **1965**, 96, 368–382.
- [9] M. S. Pilone, D-Amino acid oxidase: new findings. *Cell. Mol. Life Sci.* **2000**, 57, 1732–1747.
- [10] RCSB Protein Data Bank, www.rcsb.org/pdb/.
- [11] NP 001908, D-amino acid oxidase [Homo sapiens], www.ncbi.nlm.nih.gov/entrez/query.fcgi?CMD.
- [12] T. Hanai, Molecular Modeling for Quantitative Analysis of Molecular Interaction”, *Lett. Drug Design Discovery* **2005**, 2, 232–238.
- [13] C. M. Haris, L. Pollegioni, and S. Ghisla, pH and kinetic isotope effect in D-amino acid oxidase catalysis, *Eur. J. Biochem.* **2001**, 268, 5504–5520.
- [14] A. Mattevi, M. A. Vanoni, F. Todone, M. Rizzi, A. Teplyakov, A. Coda, M. Bolognes, and B. Curti, Crystal structure of D-amino acid oxidase: A case of active site mirror-image convergent evolution with flavocytochrome β_2 , *Proc. Natl. Acad. Sci. USA* **1996**, 93, 7496–7501.
- [15] S. Umhau, L. Pollegioni, G. Molla, K. Diederichs, W. Welte, M. S. Pilone, and S. Ghisla, The x-ray structure of D-amino acid oxidase at very high resolution identifies the chemical mechanism of flavin-dependent substrate dehydrogenation, *Proc. Natl. Acad. Sci. USA* **2000**, 97, 12463–12468.
- [16] R. Miura, C. Setoyama, Y. Nishina, K. Shiga, H. Mizutani, I. Miyahara, and K. Hiritsu, Structural and mechanistic studies on D-amino acid oxidase-substrate complex: Implication of the crystal structure of enzyme-substrate analog complex, *J. Biochem. (Tokyo)* **1997**, 122, 825–833.
- [17] S. Sacchi, S. Lorenzi, G. Molla, M. S. Pilone, C. Rossetti, and L. Pollegioni, Engineering the substrate specificity of D-amino acid oxidase, *J. Biol. Chem.*, **2002**, 277, 27510–27516.
- [18] S. Sacchi, E. Rosini, G. Molla, M. S. Pilone, and L. Pollegioni, Modulating D-amino acid oxidase substrate specificity: production of an enzyme for analytical determination of all D-amino acids by directed evolution, *Prot. Engng.* **2004**, 17, 517–525.
- [19] L. Pollegioni, W. Blodig, and S. Ghisla, On the mechanism of D-amino acid oxidase, *J. Biol. Chem.* **1997**, 272, 4924–4934.
- [20] L. Pollegioni, S. Ghisla, and M. S. Pilone, Studies on the active center of *Rhodotorula gracilis* D-amino acid oxidase and comparison with pig kidney enzyme. *Biochem J.* **1992**, 286, 389–394.

Biographies

Toshihiko Hanai is research scientist at Health Research Foundation. After obtaining Ph.D. degree in analytical chemistry from Kyoto University, Dr. Hanai undertook postdoctoral research with Professor B. Karger at Northeastern University, and with Professors H. Walton and R. Sieverse at Colorado University at Boulder. Dr. Hanai was postdoctoral research fellow then research assistant at Universite de Montreal. He was research manager at GasukuroKogyo. Dr. Hanai collaborated on pharmaceutical analysis with Professors T. Kinoshita and H. Homma at Kitasato University. Dr. Hanai published 13 scientific books including 7 books in English about HPLC. His research interesting is Chromatography and Computational Chemistry for Drug Discovery to accelerate drug discovery as an analytical chemist.